Solar Energy Advances 4 (2024) 100047

Contents lists available at ScienceDirect

Solar Energy Advances

journal homepage: www.elsevier.com/locate/seja

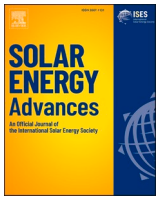

# Analysis of the performance and operation of a photovoltaic-battery heat pump system based on field measurement data

Shubham Baraskar [a,#], Danny Günther [a,*], Jeannette Wapler [a], Manuel Lämmle [a,b]

[a] Fraunhofer Institute for Solar Energy Systems ISE, Freiburg, Germany
[b] Offenburg University of Applied Sciences, Offenburg, Germany

ARTICLE INFO

*Keywords:*
Heat pump
Photovoltaic
Battery
Energy-efficiency
Monitoring
Self-consumption
Sg-ready

ABSTRACT

Photovoltaic-heat pump (PV-HP) combinations with battery and energy management systems are becoming increasingly popular due to their ability to increase the autarchy and utilization of self-generated PV electricity. This trend is driven by the ongoing electrification of the heating sector and the growing disparity between growing electricity costs and reducing feed-in tariffs in Germany. Smart control strategies can be employed to control and optimize the heat pump operation to achieve higher self-consumption of PV electricity. This work presents the evaluation results of a smart-grid ready controlled PV-HP-battery system in a single-family household in Germany, using 1-minute-high-resolution field measurement data. Within 12 months evaluation period, a self-consumption of 43 % was determined. The solar fraction of the HP amounts to 36 %, enabled also due to higher set temperatures for space heating and domestic hot water production. Accordingly, the SPF decreases by 4.0 % the space heating and by 5.7 % in the domestic hot water mode. The combined seasonal performance factor for the heat pump system increases from 4.2 to 6.7, when only considering the electricity taken from the grid and disregarding the locally generated electricity supplied from photovoltaic and battery units.

## 1. Introduction

### 1.1. Background

In Germany, the buildings sector is responsible for 35 % of the total energy consumption, 63 % of which is from the residential buildings [1]. Hence, the residential sector offers a high savings potential in the energy sector transition. More than 80 % of the residential final energy consumption is attributable to space heating (70 %) and hot water preparation (14 %) [2]. Hence, an energy efficiency improvement of the heating sector, by promoting renewable energy utilization is a viable solution for decarbonizing the buildings sector.

Heat pumps (HP) play a key role in this context. Thanks to their high energy efficiency and low emissions, heat pumps are gaining ever increasing acceptance. In the German context, the government has agreed upon the goal of commissioning 500,000 heat pumps each year from 2024 [3] whereby possibly each new heating system in the building should be operated with at least 65 % renewable energy [3,4]. In the residential sector, electrically driven compression heat pumps, particularly air source heat pumps are most employed, followed by ground source heat pumps [5]. A further savings potential lies in improving the electrical energy input to the heat pump, for example, in the form of renewable photovoltaics (PV) energy.

Rooftop PV systems are rapidly expanding not just in Germany, but also on a global scale [6]. PV systems have short payback time [6], providing both financial as well as environmental advantages. The PV production can also be fed into the electricity grid, against a remuneration in the form of feed-in tariff. In Germany, the feed-in tariff for PV systems under 10 kW became lower than the grid electricity prices in 2012, after which it became a better choice for the homeowners to self-consume their PV energy [7]. Furthermore, the recent Russia-Ukraine conflict has led to significant surge in the electricity prices [8], and the need for higher self-consumption (SC) is becoming increasingly relevant.

PV generation varies with solar irradiance, while household demand remains relatively constant throughout the day. This temporal mismatch limits the direct domestic consumption of PV electricity [7] and results in significant grid feed-in, straining the grid [9]. Electrical battery storage when coupled to the PV unit, can store the surplus PV power, and supply it to the building loads as per the demand [10].

* Corresponding author.
*E-mail address:* danny.guenther@ise.fraunhofer.de (D. Günther).
# Main author

https://doi.org/10.1016/j.seja.2023.100047
Received 29 September 2023; Received in revised form 14 November 2023; Accepted 14 November 2023
Available online 19 November 2023

Several studies mention the benefits of PV-battery systems in the form of increased self-consumption and autarchy [7,11,12]. Self-consumption describes the proportion of the total domestic PV energy production that is used directly in the building or for battery charging [13], whereas the autarchy quantifies the proportion of the total household load, which is supplied by the PV, either directly or through battery [13]. Additionally, batteries can also reduce the grid strain caused due to excessive feed-in during peak hours of PV production [9,14]. Car-charging batteries offer similar opportunity to increase the self-consumption of domestic PV generation [15]. This paper analyses one such PV-battery system in terms of its self-consumption levels, and the effect of integrating it with the heat pump unit.

The coupling of heating and electricity sectors, in the form of PV-HP systems is gaining interest from many. Smart heat pumps that can communicate with the home energy system, can adjust their operation to maximize the domestic PV consumption or operate grid-oriented, depending on the employed control strategy [16]. In this context, photovoltaic systems influence the operation of heat pumps to harness surplus available electricity. This manipulation is performed through strategies like intensified heat pump operation, increased storage set-point temperatures, or by shifting the heat pump operation depending on the available PV electricity. Such feature which allows to control heat pumps based on available electricity is the SG-Ready (short for smart grid ready) standard which is detailed in Section 2.1.1. Importantly, these strategies hold the potential to impact the operational efficiency of heat pumps. This complex interaction constitutes a key focal point that this study aims to explore. Several studies discuss the strength of PV-HP systems, such as increased self-consumption and grid independence, in addition to the economic and environmental benefits [16,17,18,19,20,21,22]. Fischer et al. [22] show the load-shifting potential by analyzing a pool of 284 heat pumps in terms of their response to different SG-Ready signals, with the help of simulations. They show that load-shifting leads to significant energy losses in the heat pump system. In [20], authors simulated a PV-HP system with electrical and thermal storages and confirmed that smart heat pump control strategies help in reducing the power purchased from the grid by shifting operation to hours with PV surplus power and overheating the DHW storage tank.

In a general context, if one does not consider the investment, maintenance, and possible insurance costs, the electricity from the PV and the battery are free for the user, as opposed to continuous costs of purchasing grid electricity. Hence, it becomes interesting to analyze the heat pump performance only for the grid electricity supplied. By considering electricity savings due to PV and battery power supplied to the heat pump, the performance factor can be calculated for only the grid electricity input to heat pump for the same heat output. Certain energy performance factors for PV-HP systems which consider only the grid electricity supplied to the heat pump system, have been mentioned in Report D1 of the SHC Task 60 [23]. Niederhäuser et al. [18] performed a monitoring study for a PV-HP combination, where the complete PV power was supplied to the heat pump. Authors observed that for the same system boundary (including heat delivery side), considering the PV production increased the seasonal performance factor (SPF) from 5.3 to 6.9. Fraga et al. [24] showed the benefit of PV supply to heat pump in the form of significantly high SPFs (up to 21.9) for a new building with a water-source heat pump for various retrofit states of a building. In their comprehensive review of solar-heat pump systems, Poppi et al. [17] discussed the importance of proper definition of system boundaries when considering PV-HP systems. They further discuss the importance of higher time resolution, and the added complexity in evaluating the PV-HP systems, when a battery supply to the heat pump and other building loads is additionally considered. In this regard, a clear definition of system boundaries is crucial for PV-HP-battery systems [17]. The system boundaries are the basis for evaluation of heat pump systems, which govern the interpretation of the associated key performance indicators (KPIs). According to Poppi et al. [17] a common practice in this respect could not be identified, and more work needs to be done for evaluating the benefits of PV-HP system combination.

### 1.2. Objective and structure

Several studies have taken experimental or simulation-based approach to gain insights into the PV-HP combination in terms of system combinations, smart control of heat pumps, grid-supportive operation, and the ecological and economic impacts of such combinations [16,17,18,19,20,21,22]. However, in-depth research is missing in terms of the impact of smart control on the dynamic performance efficiency of the heat pump. Moreover, extensive work needs to be done to analyze the effect of PV and battery units on the energy consumed by the heat pump by redefining the system boundaries of the PV-HP systems.

This work aims to support the ongoing research on PV-HP systems in combination with battery units. Real-world data from a single-family house in the Freiburg, Germany was collected with the help of the installed measurement equipment and analyzed to evaluate the system performance. The evaluation outcomes of the system are presented in the form of various KPIs, by addressing the following research question:

- How do the PV and battery units affect the performance of the solar heat pump system?
- How does the smart control affect the operation behavior and efficiency of the heat pump?

Section 2 delves into the methodology, providing a detailed account of the system's setup, encompassing both the hydraulic and electrical connections. After a description of the SG-Ready control, the energy management sequence of the PV-HP system is also described, accompanied by the establishment of a set of KPIs to quantify the system performance. Section 3 presents the evaluation results of the system's performance. Furthermore, the impact of the SG-Ready smart control on heat pump supply temperatures is also discussed here. The discussion in Section 4 critically analyzes the results in the context of the research questions posed at the outset and is pivotal in terms of interpreting the significance of the findings and offering insights into the broader context of the study. The key findings of this work are summarized in Section 5, conclusion.

## 2. Methodology

### 2.1. System description

The analysis performed in this study is based on field-measurement data from a semi-detached house located in Freiburg, Germany. The house was built in 1960 and has a heated living space of 256 $m^2$. The house has an annual specific heating demand of 84.3 kWh/$m^2$a.

The hydronic components installed in the system are shown in Fig. 1. The system is composed of a ground source heat pump with a nominal capacity of 13.9 kW (B0/W35) which extracts heat from the ground via a single borehole heat exchanger. The heat generated by the heat pump is utilized for room heating through buffer storage and for domestic hot water preparation via a storage tank and a freshwater station. Both the storages are equipped with electric auxiliary heaters. The thermal output of the auxiliary heaters is set to be computed by the data acquisition (DAQ) unit from the measured electrical consumption considering a conversion efficiency of 100 %. However, from monitoring it was observed that the auxiliary heaters were inoperative for the complete monitoring period, and the complete thermal energy was provided by the heat pump.

Heat meters are placed at various locations in the circuit as indicated by the green boxes. Directly downstream the heat pump, a single heat meter measures the heat output of the heat pump, while the separation between space heating and DHW modes is done by measuring the state of the control valve. The heat meters measure the difference between the

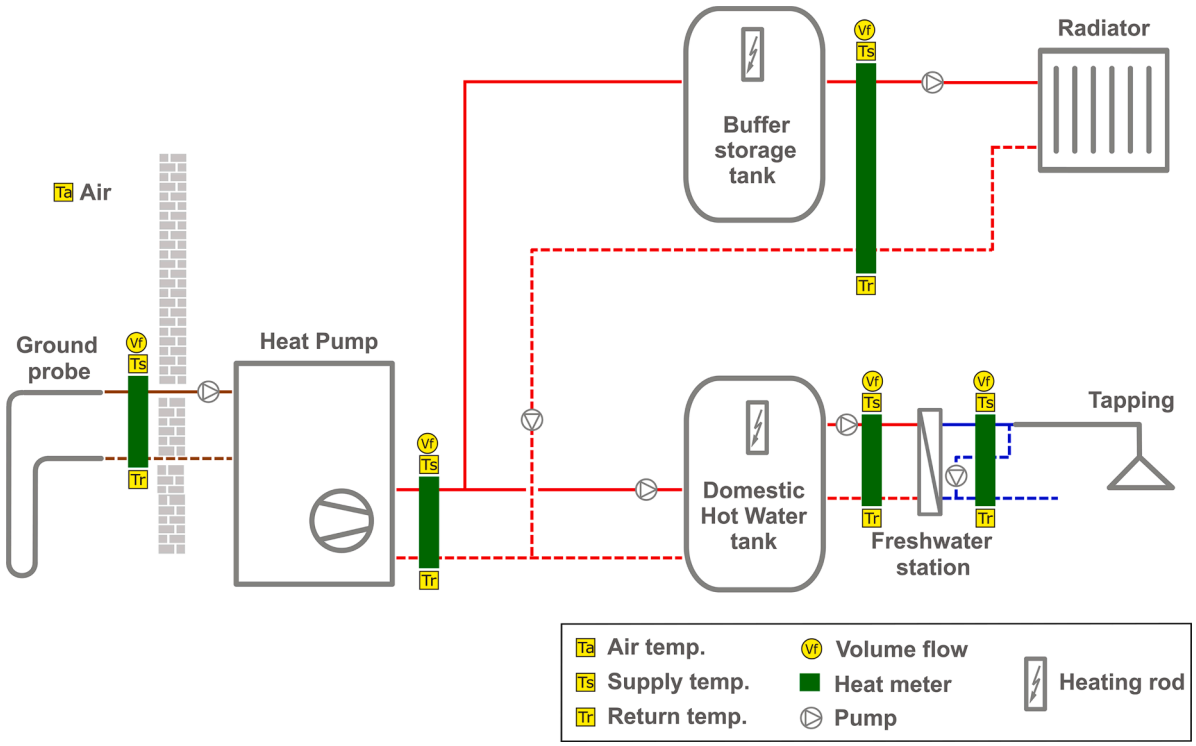


**Fig. 1.** Hydronic system connections for the system.

supply and return temperatures; and together with the measured volume flow, calculate the thermal energy at the locations as indicated in the figure.

Fig. 2 shows the electrical components in the system. On the electrical side, the on-grid PV array, supplemented by the battery unit, is the primary supply source for the household followed by grid purchase. The system has a PV unit with a module area of 60 $m^2$ and nominal power of 12.3 kWp. The PV module is oriented in the South-Southwest direction and has a tilt of 30° The DC-coupled electrical battery storage unit has a capacity of 11.7 kWh. The DC power from PV and battery units is converted to AC via an inverter which has a maximum AC power of 12 kW and a European efficiency of 95 %.

### 2.1.1. SG-Ready control of heat pumps

Heat pumps with SG-Ready (smart grid-ready) labels can interact with the electricity grid and correspondingly adjust their operation in a grid-oriented way [25]. During the periods of high grid load, the grid operator can turn off the heat pump operation to reduce the grid strain

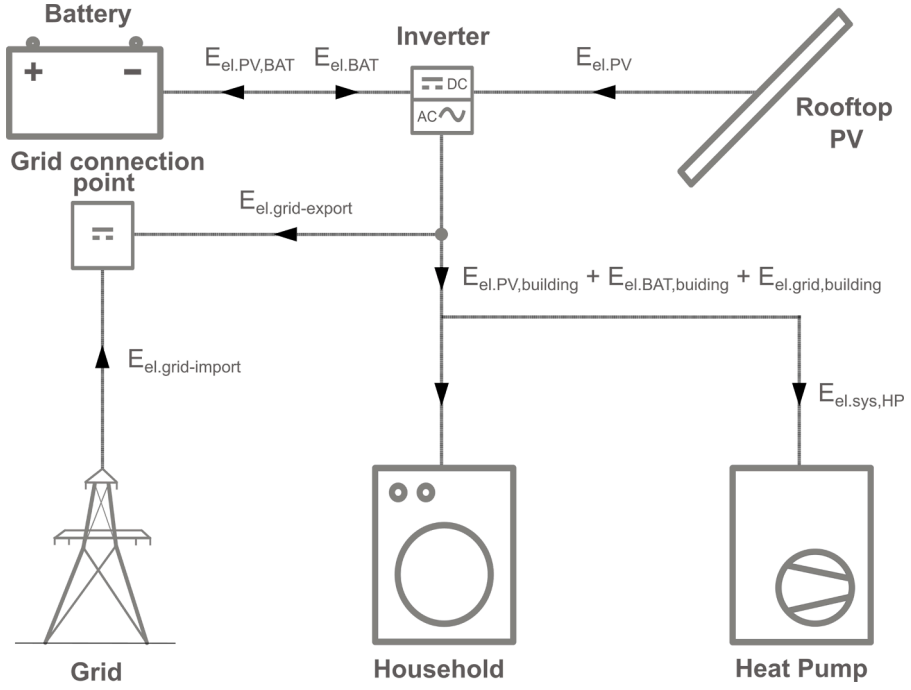


**Fig. 2.** Electrical connections for the system.

or can also undergo a forced turn on in the opposite case. This can serve to influence the electrical load, for instance, to stabilize the overall load and/or prevent the curtailment of wind or PV power generation. Similarly, the SG-Ready interface can also be utilized to maximize the PV self-consumption by adjusting the heat pump operation based on available PV electricity [25]. The SG-Ready label helps to identify heat pumps that have the capability to operate over the following operation states [22,25]:

**Table 1**
SG-Ready operation states [22,25].

| Operation State | Description |
|---|---|
| OS1: Forced OFF | HP is switched off, for a maximum of 2 hours |
| OS2: Normal operation | Unaffected operation, obeying the set system limits |
| OS3: Recommended ON | Boosted HP operation for space and domestic hot water heating.<br>Recommended switch-on command. |
| OS4: Forced ON | Variant 1: HP actively switched on<br>Variant 2: HP and auxiliary heater actively switched on<br>Optional: increased storage temperatures |

### 2.1.2. Energy management sequence

The control sequence of the commercial energy management system is obtained from analyzing the field data (refer Fig. 3): PV power is prioritized for building loads to maximize the self-consumption. Any surplus power is used to charge the battery, considering its state of charge (SOC). If PV power exceeds the maximum battery charging power or storage capacity, the excess power is exported to the grid. If PV power is insufficient to meet building load requirements, power is drawn from the battery. If the battery is empty or already discharging at maximum power, any remaining instantaneous demand is fulfilled through grid supply.

The heat pump is controlled over the SG-Ready interface which modifies the heat pump operation to maximize PV self-consumption. In the analyzed system, the SG-Ready is configured to trigger the heat pump in boosted operation, whereby the space heating and DHW supply temperatures are increased. This corresponds to the state OS3 as described in Table 1. The SG-Ready mode is activated when the battery is fully charged or is charging at its maximum power and there is still PV surplus available. Conversely, the trigger-off condition is met when the instantaneous PV power remains lower than the total building demand for at least 10 min. For the studied system, the trigger off corresponds to state OS2, where the heat pump is sent back to normal operation, obeying the set system parameters.

## 2.2. Data processing

In this section the methodology applied for evaluating the residential energy systems is explained. The thermal and electrical data of the systems, as outlined in Table A.1 (appendix) was collected from 01.01.2022 to 31.12.2022. The evaluated system was equipped with monitoring equipment which collected the data pertaining to thermal and electrical characteristics of the system. Details regarding the measurement equipment is mentioned in Table A.2. The data acquisition (DAQ) unit gathered the data at a high-resolution of 10 s and utilized the modbus communication protocol to transfer daily raw data to a Fraunhofer ISE server. This collected data was further read into mondas® where further processing and monitoring was performed. mondas® is an IoT web platform used for real-time data management, data analysis (error detection, calculation, data filtering, etc.), and visualization.

For analysis, 1-minute resolution data was exported from mondas®, where the conversion from 10 s to 1 min resolution was achieved by computing the mean of the raw data over each minute for power data. The next step involved checking the data against logical limits and comparing it with the component parameters provided by the manufacturers. Any outlying data, resulting from failure of the DAQ unit or faulty measurements by the sensors, for example, a sudden 0 instantaneous value for the building consumption, was masked to ensure correctness of the subsequent evaluation. Next, the system power balance was assessed by comparing the system's power inflows and outflows for each minute. Adopting a similar approach, the balance was performed

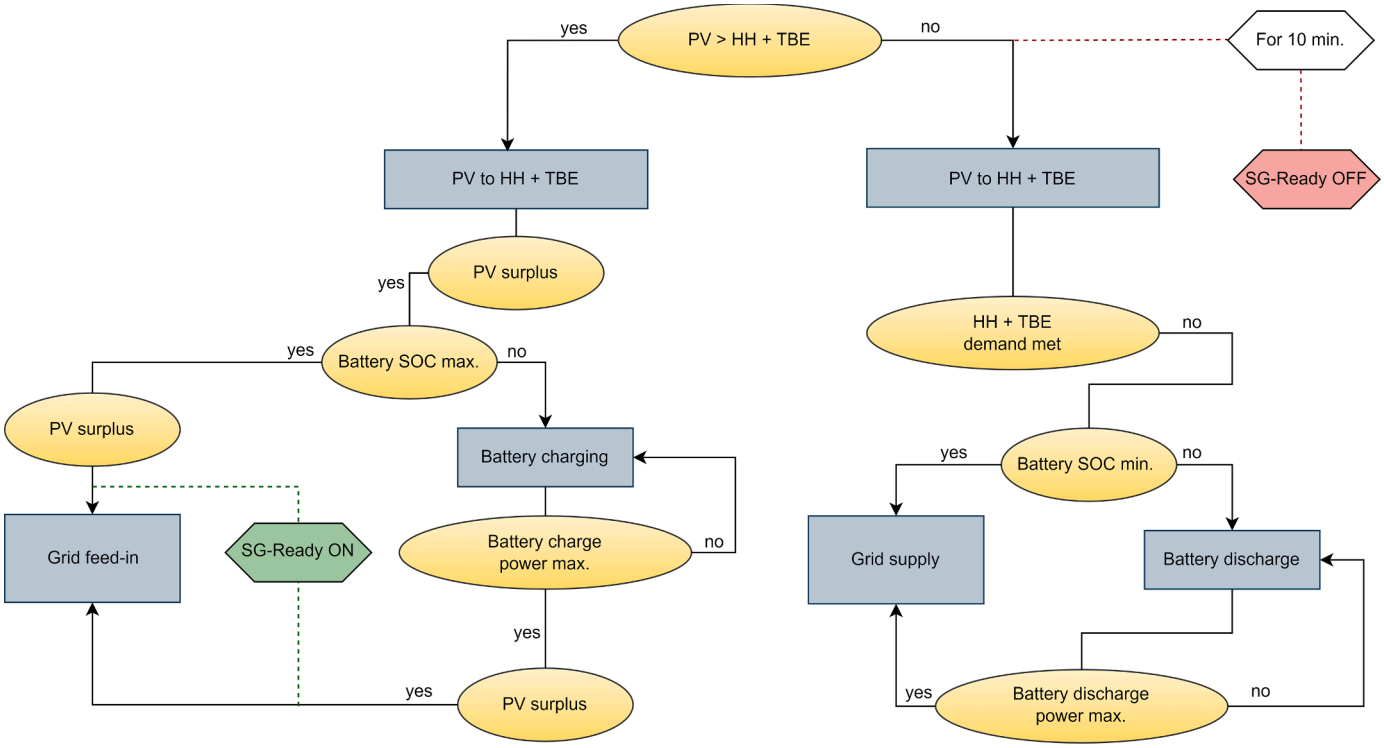


**Fig. 3.** Energy management sequence.

for daily, and monthly timescales. Table A.5 (appendix) mentions the components considered under the input and output power flows.

### 2.3. Key performance indicators (KPIs) for PV-HP-battery systems

KPIs are crucial when analyzing the performance of the system. The following set of KPIs was selected based on previous studies allowing a consistent description of the electrical and thermal performance of the PV-HP battery system in the building context. After the data processing and plausibility check, the system was evaluated by calculating the KPIs as follows, using electricity E and heat Q according to the nomenclature shown in Fig. 4:

- Self-consumption: Self-consumption gives the proportion of the total domestic PV energy production that is directly used by the building loads ($E_{el.PV,building}$) or in the form of battery charging ($E_{el.PV,BAT}$). Low values of self-consumption indicate a high grid feed-in.

$$SC = \frac{E_{el.PV,building} + E_{el.PV,BAT}}{E_{el.PV}} \quad (1)$$

- Solar fraction: in the context of the heat pumps, solar fraction refers to the ratio of PV electricity supplied directly to the heat pump load ($E_{el.PV,HP}$) or through battery discharge ($E_{el.BAT,HP}$), to the total heat pump electricity consumption ($E_{el.sys,HP}$).

$$SF = \frac{E_{el.PV,HP} + E_{el.BAT,HP}}{E_{el.sys,HP}} \quad (2)$$

- Seasonal performance factor: SPF is the ratio of total thermal energy delivered by a heat pump during a heating/cooling season or over a year to its electrical consumption during the same period. The interpretation of SPF is subject to the definition of system boundary (SB). The boundary specifies the components for which the thermal and electrical parameters are included for calculating the SPF. The analysis in this work is based on system boundary 3 according to a field measurement project, WPsmart im Bestand [26], which includes the auxiliary heater along with the heat pump compressor, source side pump, and the controls (refer Fig. A.1 and Table A.6; appendix).

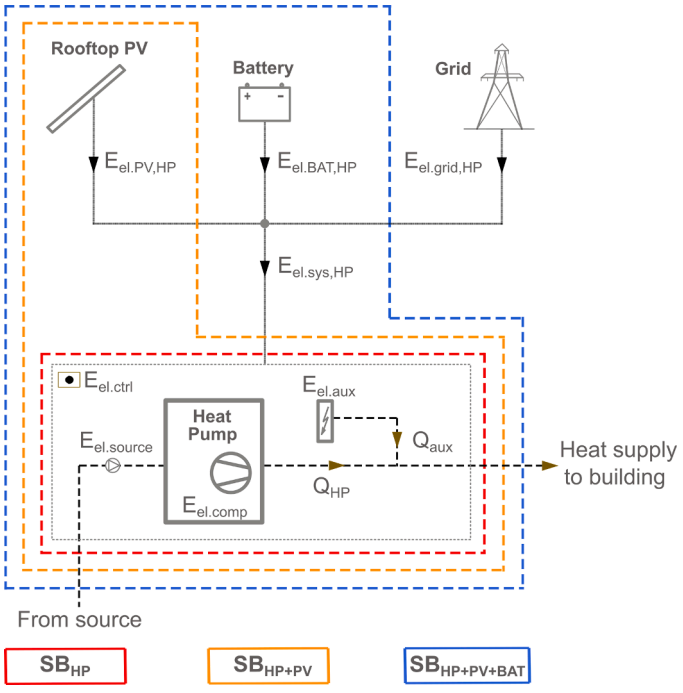


**Fig. 4.** Illustration of system boundaries by considering PV and battery supply to the heat pump.

The SPF is similar to coefficient of performance (COP) in that both the parameters give the efficiency of the heat pump. However, COP can be understood as an efficiency value that is valid for fixed boundary conditions (for example A2/W35). Whereas SPF is the efficiency over a longer period (complete year, or a heating/ cooling season), with varying boundary conditions.

$$SPF3 = \frac{Q_{HP} + Q_{aux}}{E_{el.comp} + E_{el.aux} + E_{el.source} + E_{el.ctrl}} \quad (3)$$

- Heating curve: The heating curve of a heat pump gives the relationship between the outside air temperature and the required supply or return temperature for space heating in order to meet the required heat demand [27]. The heat pump controller determines the space heating supply or return temperature of the heat pump based on the measured ambient temperature [27,28]. If the outside temperature increases, the flow temperature of the heat pump reduces and vice-e-versa. Excessively high temperatures in the heating circuit can lead to heat losses. Hence, the heating curve controls the flow temperatures accordingly to fulfill the building's heating demand. In practice, the heat pump controllers apply a moving average of a certain time to dampen the ambient temperatures and to increase robustness of the system [28].

According to [17,23], it can be useful to evaluate the performance of the heat pump for only the electricity consumed from the grid for heat pumps combined with PV systems. This approach is grounded in the assumption that electricity generated by domestic PV and battery units is effectively cost-free for homeowners. Consequently, the focus shifts to quantifying the heat output produced by the heat pump per unit of grid electricity purchased. To further analyze the effect of PV and battery on the performance of the heat pump, the SPF3 is calculated for three different system boundaries as illustrated in Fig. 4. Only the components outside the boundary are considered as electricity sources. For system boundary $SB_{HP}$, only the heat pump is considered inside the boundary, and the total consumption of the heat pump is accounted for. The corresponding $SPF3_{HP}$ is the conventional SPF3 of the system. For $SB_{HP+PV}$, the direct supply of PV to the heat pump is not considered since it is generated inside the system boundary, and the corresponding SPF3 is $SPF3_{HP+PV}$. Similarly, for boundary $SB_{HP+PV+BAT}$, only the grid electricity supplied to the heat pump is considered for calculating $SPF3_{HP+PV+BAT}$, giving value to the complete locally generated electricity of the PV+battery system.

If the total electricity supplied to the heat pump is referred to as $E_{el.sys,HP}$, where:

$$E_{el.sys,HP} = E_{el.grid,HP} + E_{el.PV,HP} + E_{el.BAT,HP} \quad (4)$$

Then, for the boundary $SB_{HP}$, considering the total electricity supplied to the heat pump, $SPF3_{HP}$ is given by:

$$SPF3_{HP} = \frac{Q_{HP} + Q_{aux}}{E_{el.sys,HP}} \quad (5)$$

For boundary $SB_{HP+PV}$, considering self-consumption of PV, $SPF3_{HP+PV}$ is calculated as:

$$SPF3_{HP+PV} = \frac{Q_{HP} + Q_{aux}}{E_{el.sys,HP} - E_{el.PV,HP}} \quad (6)$$

Finally, for the boundary $SB_{HP+PV+BAT}$, considering self-consumption of PV and battery, $SPF3_{HP+PV+BAT}$ is determined by:

$$SPF3_{HP+PV+BAT} = \frac{Q_{HP} + Q_{aux}}{E_{el.sys,HP} - E_{el.PV,HP} - E_{el.BAT,HP}} \quad (7)$$

## 3. Results

This section discusses the evaluation outcomes from the analyzed building where the conclusions have been drawn by analyzing 1-minute resolution field data. The results are discussed with regard to the above-mentioned KPIs. For a better interpretation of the results, it must be considered that the global solar radiation at the Freiburg site in 2022 (1348 kWh/m$^2$) was 9.3 % above the average for the period 2013 to 2022 (1234 kWh/m$^2$), based on measurement data from the own Fraunhofer ISE weather station.

### 3.1. Self-consumption (SC) of the PV system

Fig. 5 shows the monthly data points for PV self-consumption, depicted by the red markers. Corresponding energy metrics are displayed through bars, where the blue segment signifies locally utilized PV-generated electricity, and the orange portion represents electricity exported to the grid during each month over the observed period. The illustration reveals distinct opposing annual trends in PV generation and self-consumption. During winter months (November - February), self-consumption exhibited elevated levels, ranging between 94 % and 100 %. This phenomenon can be attributed to diminished PV generation during winter, with most of the generated energy directly serving to household demands. In contrast, in the months spanning from May to August, characterized by substantial monthly PV generation exceeding 1600 kWh, self-consumption remained low, staying below 50 %. This was due to the surplus electricity that had to be redirected to the grid. Notably, July registered the lowest self-consumption at 25 %, having the highest PV generation of the year at 1755 kWh.

The relationship between PV generation and self-consumption is effectively showcased through carpet plots, as illustrated in Fig. 6. It might be tempting to consider the PV system oversized or the battery undersized for the summer season, and vice versa for the winter months. However, determining the optimal component sizes needs meticulous calculations, considering both the energetic and economic aspects.

Fig. 6 shows the annual character of PV generation and the corresponding self-consumption in the form of carpet plots. The x-axis represents the months of the observation year while the y-axis represents hours of the day. In the first graph 'PV generation', the red regions show high PV power being generated between the hours of 10:00 AM and 06:00 PM and during the months of March through September where the instantaneous PV power is more than 5 kW. This pattern diminishes towards the winter months and towards the end of the day as the PV generation is low. Correspondingly, the 'SC' to the right shows the annual pattern in the self-consumption for the PV system. In contrast to the timeframe with high PV generation, low values of SC can be observed. In this region, the SC maintained below 50 %, indicative of a high grid export. Correspondingly, the initial and final months of the year relate to very high self-consumption levels with values reaching 100 %, as the low PV power generated during period is to a great extent directly used by the building loads. Moreover, higher HP consumption due to increased space heating demand in Winter further adds to the high SC values. Calculated from the sum of energies, the system has an annual self-consumption of 42.9 %.

### 3.2. Solar fraction (SF) of the heat pump system

The solar fraction of the heat pump is shown in Fig. 7. The height of the bars represents the total consumption of the heat pump for each month of the year, whereas the orange, blue, and gray sections of the bars represent the supply from the PV, battery, and grid respectively. The annual behavior of energy consumption is clearly visible where the heat pump consumes little electricity in the warmer months from May to October, and more during the other months due to increased space heating demand. This results in a similar, yet opposite pattern followed by the solar fraction of the heat pump, as indicated by the red markers. The very high solar fraction, greater than 0.90, from June through August can be explained by the reduced heat pump electricity demand due to DHW-only operation of the heat pump. This is directly related to the high PV generation during this period where the heat pump could directly consume the PV electricity. Additionally, the smart control of the heat pump through SG-Ready interface intensified the heat pump operation which concentrated the operation in the hours of PV

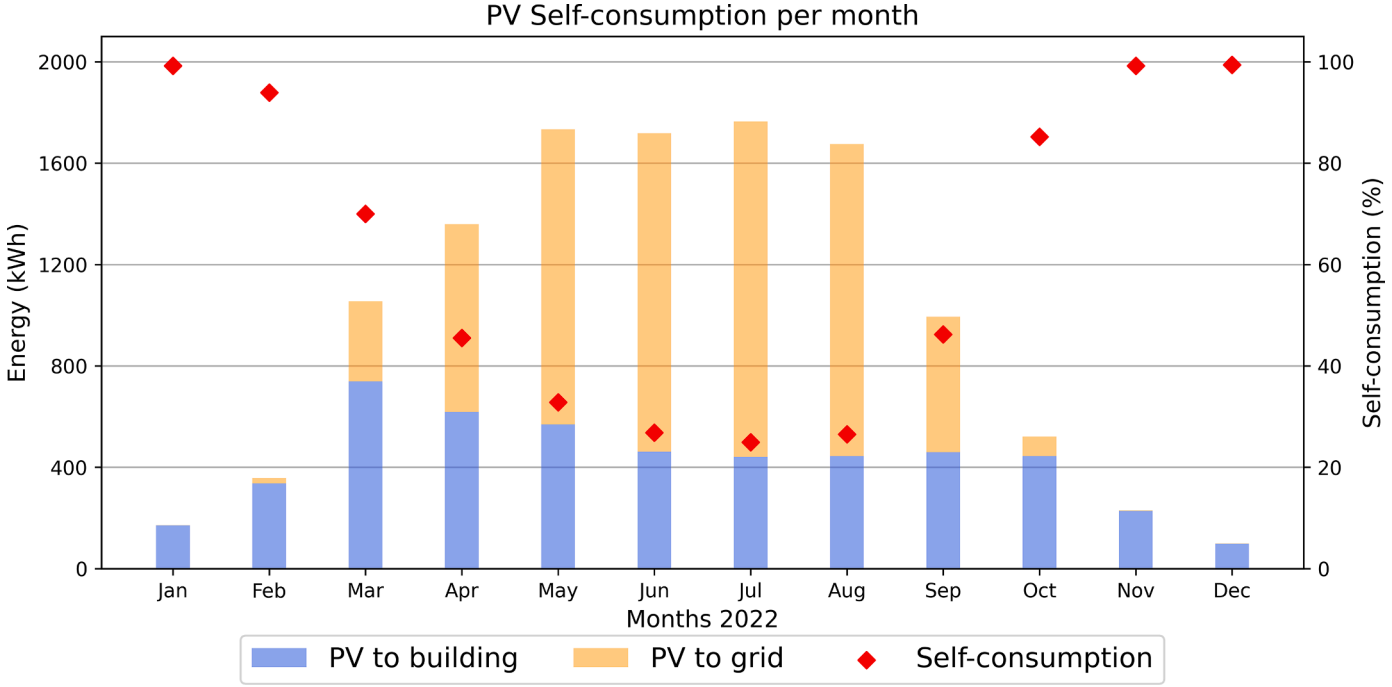


**Fig. 5.** Monthly energy generated by the PV and self-consumption (SC) of the system for the entire observation period.

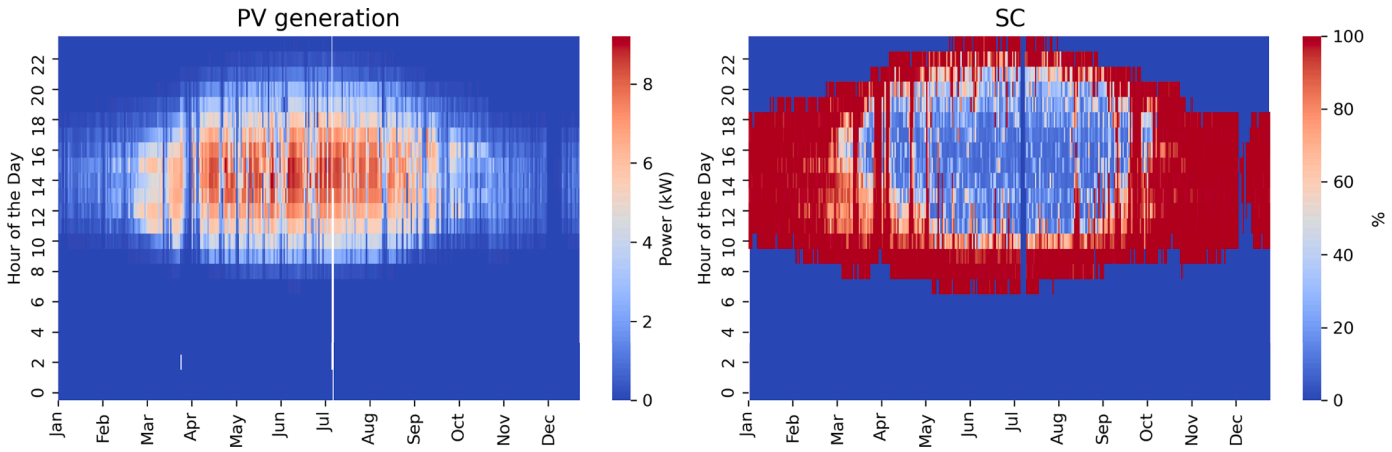


**Fig 6.** Annual behavior of PV generation and the corresponding self-consumption.

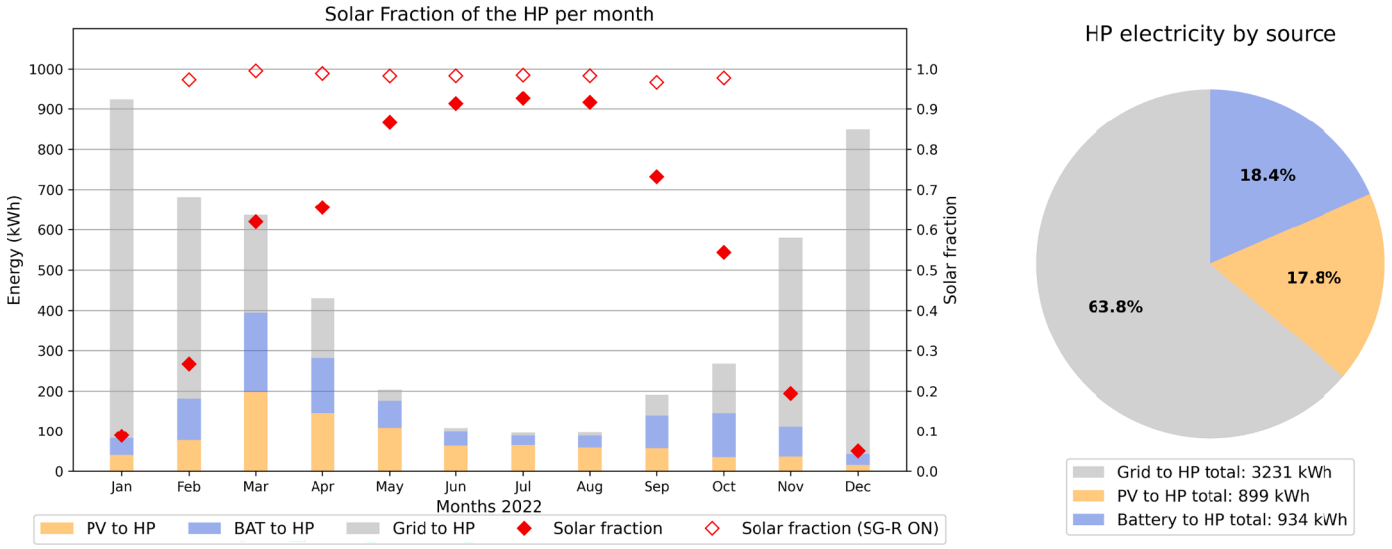


**Fig 7.** Monthly energy consumption and solar fraction (SF) of the heat pump (left) and the percentage contribution of different electrical sources to the annual heat pump electricity consumption (right).

availability, further adding to the solar fraction. The opposite effect can be seen for the months January-February and November-December, where the comparatively lower PV generation limited the solar fraction to a maximum of 0.26 while being the lowest at 0.05 in December.

For a comparative analysis, the hollow markers indicate solar fraction of the heat pump for the times when the SG-Ready mode actively controlled the heat pump operation. During these times, a very low amount of energy had to be supplied from the grid, and a high solar fraction was achieved. Computed by summing the energies for the whole year, the system had an annual solar fraction of 0.36, compared to 0.98 during the times with SG-Ready signal on.

The pie chart to the right (Fig. 7) graphically represents the shares of the available electricity sources for the heat pump. The share of PV and battery supply to the heat pump are similar over the year. However, the contribution of PV energy appears to dominate during May to August, while in the later months the battery supplied more energy to the heat pump than the PV. This is because during the colder months, the increased space heating demand, with lower levels of irradiance results in a mismatch of PV generation and heat demand. Overall, during the evaluation period, the heat pump consumed a total of 5064 kWh of which a major 63.8 % was contributed by grid supply. The PV array supplied 899 kWh (17.8 %), and the battery unit supplied 934 kWh (18.4 %), resulting in an annual solar fraction of SF = 0.36. These shares are represented graphically by the pie chart in Fig. 7.

### 3.3. Seasonal performance factor (SPF3) by source of electricity

Corresponding to the different system boundaries for PV-HP-battery systems (refer section 2.2.2), Fig. 8 represents the SPF3 for different system boundaries on the electrical side, the corresponding electricity consumption, and the thermal energy generation of the heat pump. To estimate the effects of the measurement accuracy on the SPF3, Tables A.3 and A.4 contain a corresponding calculation according [26]. Based on the assumed operating conditions the relative error of the SPF3 amounts to 4.4 %. The three boxes on the left show the electrical consumption of the heat pump, whereas the orange bar to the right represents the total thermal output of the heat pump for space heating and DHW. The total electrical consumption for the boundary $SB_{HP}$ is represented by the red area, and the marker shows the corresponding $SPF3_{HP}$. The $SPF3_{HP}$ of 4.2 is calculated based on the total electricity consumption of the heat pump, irrespective of the source and by assuming that the complete electricity is supplied by the grid. This implies that for each kWh of grid energy purchased, the user received 4.2 kWh of thermal energy.

Similar illustrations for boundaries $SB_{HP+PV}$ and $SB_{HP+PV+Bat}$ are made by the yellow and the blue areas respectively. When the direct

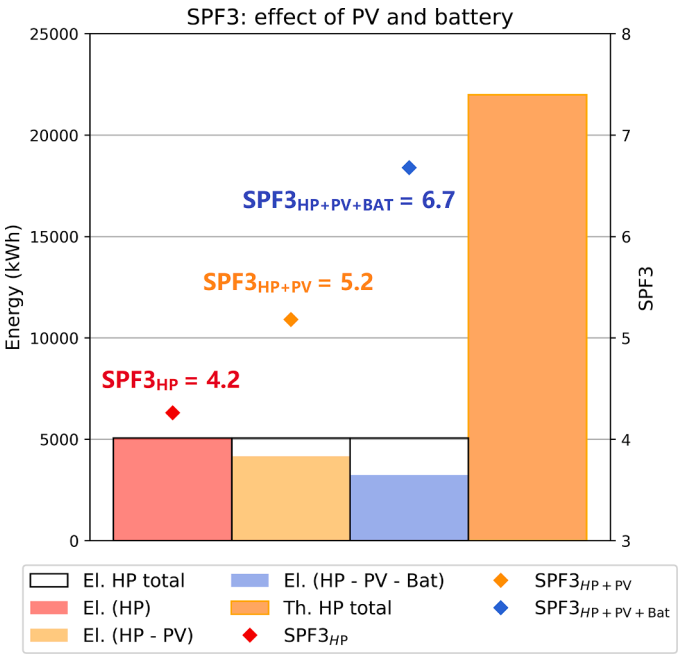


**Fig. 8.** Annual electricity consumption of the heat pump per electricity source and the corresponding SPF3.

consumption from the PV unit for the heat pump is subtracted, the SPF3 increases from $SPF3_{HP} = 4.2$ to $SPF3_{HP+PV} = 5.2$. When the electricity supplied by the battery directly to the heat pump is also considered, in addition to direct PV supply, the performance improves to $SB_{HP+PV+Bat} = 6.7$; an increase of 59.5 % compared to $SPF3_{HP}$. For the homeowner, this translates to 6.7 kWh of heat while having to pay for 1 kWh of electricity purchased from the grid.

### 3.4. *Effect of PV-optimized HP control*

Fig. 9 shows the relation of heat pump supply temperatures according to the SG-Ready states, separated for space and domestic hot water heating modes. The heat maps give an overall picture of the system operation for the whole year, where the x-axis indicates the days of the year 2022, while the y-axis represents the hours of the day. The two upper plot shows the existing relation between the PV power and SG-Ready active signal. As mentioned in Section 2.1.2 only one SG-Ready state (1) is applied to force HP operation. As it can be inferred from the plot 'PV generation', PV power was highly concentrated in the hours between 10:00 AM and 06:00 PM, and during the warmer months from March through September, with low production during the other months. Correspondingly, the system operated in the SG-Ready *on* mode for a significant share of the year. As evident from the plots 'PV generation' and 'SG-Ready status', the trigger *on* was highly dependent on the available PV power. The exact boundary conditions which triggered the SG-Ready mode, as identified from monitoring data, have been described in Section 2.2. The SG-Ready mode was greatly active in the months from February through October.

Obeying the trigger boundary conditions, the heat pump operated in SG-Ready mode for DHW preparation between February (17.02.2022) and October (16.10.2022). From the plot 'Supply temp. (DHW)' (Fig. 9), the effect of SG-Ready mode is clearly visible in terms of increased heat pump supply temperature. During the period, when the heat pump

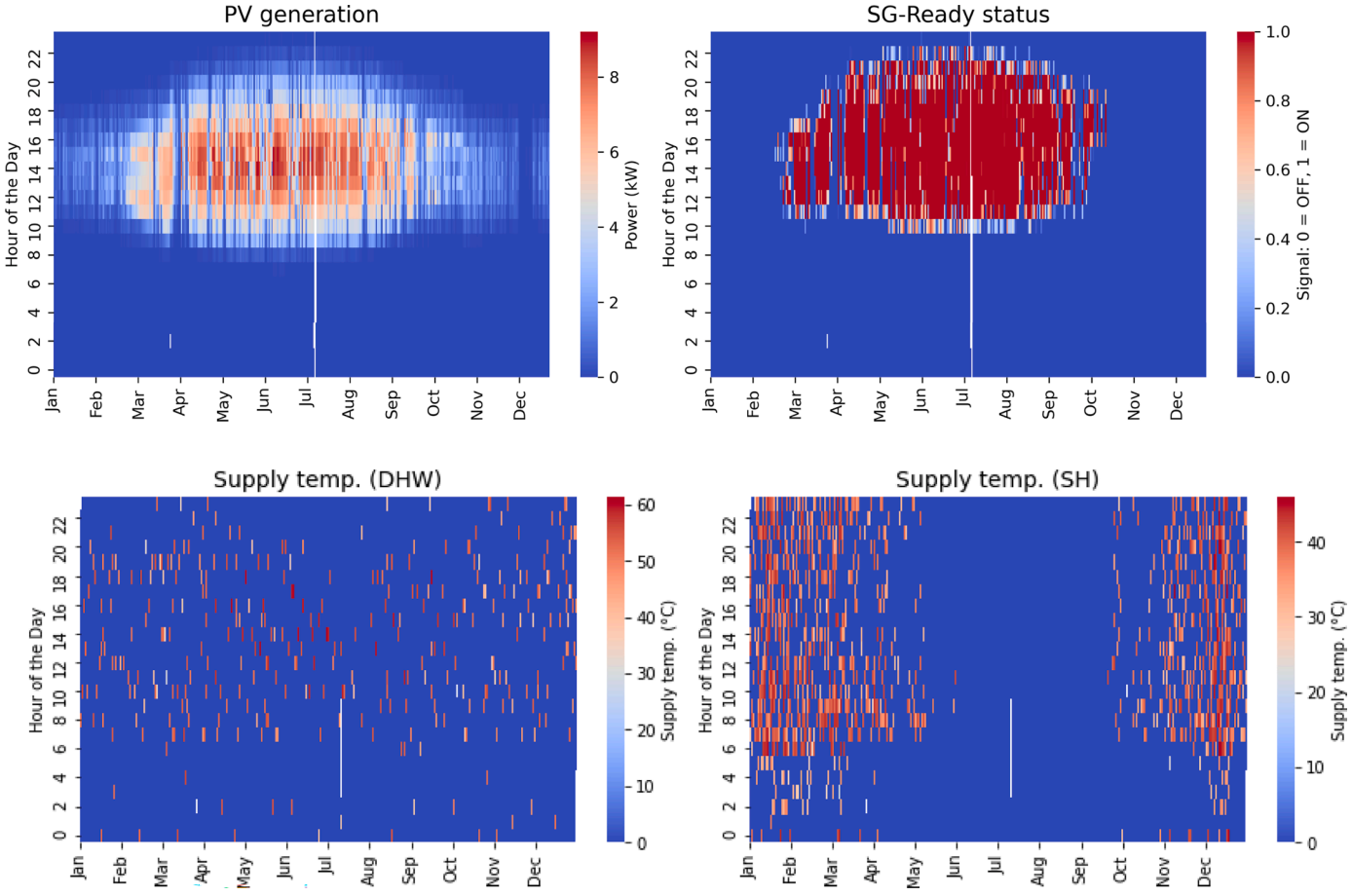


**Fig. 9.** Annual and daily PV-Power and behavior of SG-Ready signal as well as its effect on the space heating and DHW supply temperatures.

functioned under OS3, the maximum heat pump supply temperature for DHW reached to more than 60 °C, depicted by dark red regions. In contrast, the supply temperatures during the normal OS2 operation reached about 55 °C.

A similar effect was observed for space heating operation. The SG-Ready mode controlled the heat pump in space heating mode during February (19.02.2022) through October (09.10.2022). Due to comparatively warmer ambient temperatures during these months, the frequency of heat pump operation in space heating mode was low, and the effect of SG-Ready mode is not clearly visible in the plot 'Supply temp. (SH)'. However, this effect can be better observed with the measured heating curve as shown in Fig. 12 which denotes the highest supply temperatures for each space heating heat pump cycle.

### 3.4.1. *Effect of PV-optimized HP control on domestic hot water mode*

The first plot in Fig. 10 shows the maximum heat pump supply and corresponding return temperatures reached, per DHW cycle. The blue and green points represent the supply and return temperatures for OS2, whereas the respective parameters for OS3 are represented by the red and orange markers. A clear distinction can be seen between the normal (OS2) and the boosted (OS3) HP operation. The annual thermal energy weighted supply temperature is found to be 51.8 °C for OS2 and 55.5 °C for SG-Ready mode OS3; an increase of 3.7 K. Regarding the maximum supply temperatures per cycle an annual average value of 55.8 °C was determined for SG-Ready OS2, while it increased by 4.2 K to 60.0 °C under SG-Ready OS3. The temperature difference of around 5 K between the supply and return temperatures is valid for both normal and SG-Ready controlled cycles. As calculated from the regression curves for the supply temperatures for OS2 and OS3, and for the ambient temperatures between 2 °C and 35 °C, it is observed that the OS3 increases the maximum heat pump supply temperature for DHW on an average, by 4.1 K. The temperature range between 0 °C and 35 °C was chosen as both

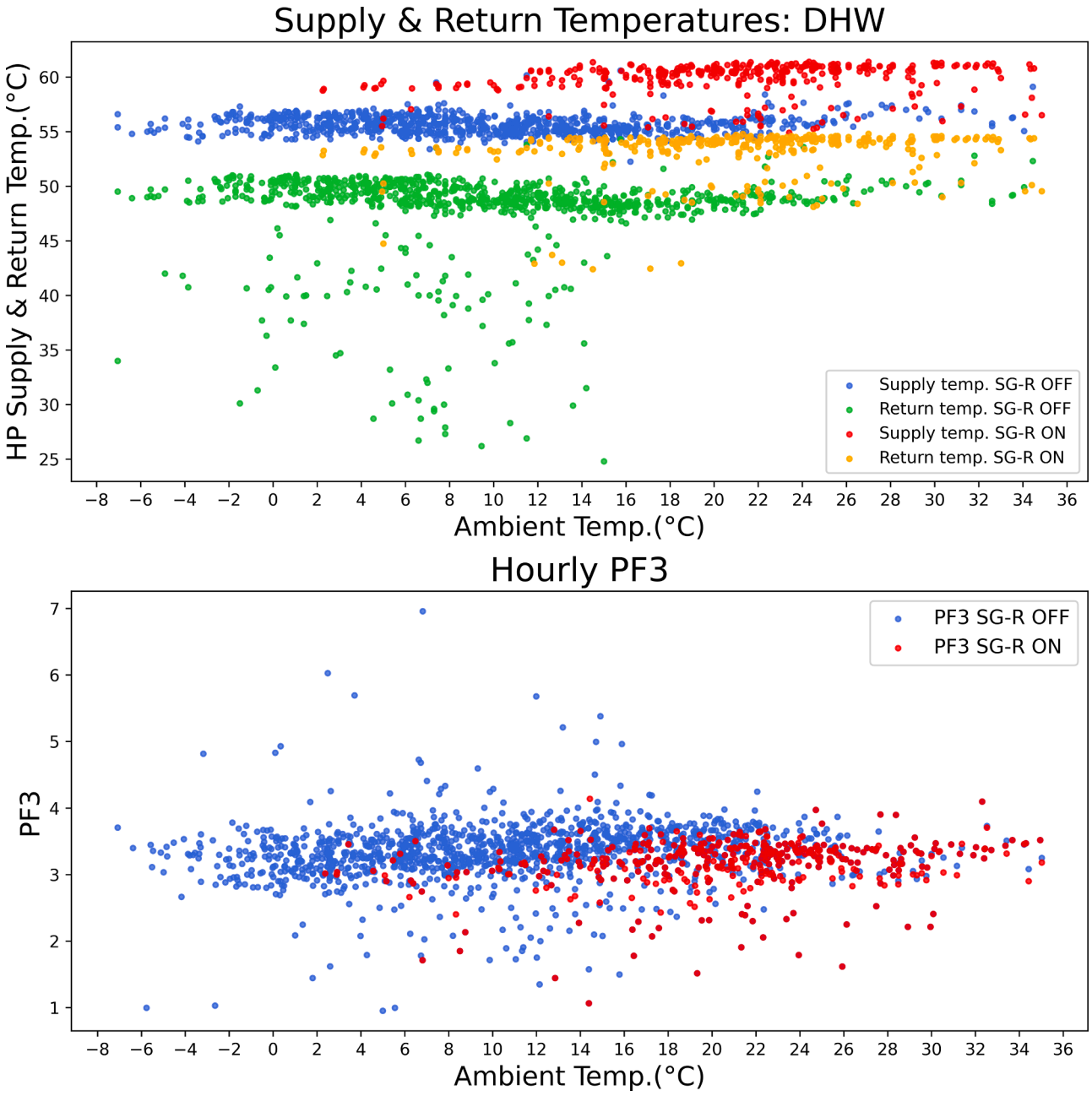


**Fig. 10.** Measured maximum supply and return temperatures per heat pump cycle vs. ambient temperature (top) and hourly PF3 vs. ambient temperature (bottom) for DHW; separated for normal and SG-Ready controlled operation.

OS2 and OS3 occur during these ambient temperatures, and hence, it makes more sense to analyze the effect for the given temperature range. More details follow in Fig. 11.

The second graph shows the hourly performance factor (PF) for DHW cycles against the ambient temperature. Neglecting the outliers, the PFs in normal operation (blue dots) were found to lie mostly between 2.6 and 4.0 with an obvious correlation to the ambient temperature, since the lower ambient temperatures lead to higher space heating demands and subsequently higher heat extraction from the ground source. This results in lower source temperatures and lower efficiency values. The PF values during SG-Ready OS3 are between 2.8 and 3.6, thus within the range of the PF with OS2, although the heat source temperatures during OS3 are higher, since those heat pump cycles for DHW are more apparent at higher ambient temperatures. In this respect, the relation of thermal energy with the ambient temperature and the corresponding effect on performance factors is better detailed in Fig. 11.

To better interpret the effect of higher supply temperatures in SG-Ready OS3 on the PF of the heat pump, the PFs in the two modes were compared for various ambient temperatures by binning them in steps of 2 K, as shown in Fig. 11. The bars represent the thermal energy produced by the heat pump for DHW in each bin; the blue section of the bars show the thermal energy generation in OS2. That in OS3 is represented by the red section. Similarly, the blue and red markers show the PF for DHW per bin, for OS2 and OS3 respectively. Over the year, the heat pump generated 5244 kWh heat for DHW preparation where more than 85 % of it occurred between the ambient temperatures of 0 °C and 24 °C. The thermal energy produced in the SG-Ready OS3 operation occurred predominantly at higher temperatures, where 96 % of the energy was generated at temperatures above 10 °C. The share of thermal energy produced under SG-Ready OS3 was found to be 1368 kWh, which accounts for 26 % of the total heat produced for DHW operation. To assess also the overall thermal energy produced with PV/Battery electricity (not shown in Fig. 11) a solar fraction of 0.51 for DHW was calculated. However, SG-Ready OS3 occurred only when the trigger conditions, mentioned in Section 2.1.2 were met.

It is a well-established understanding that the performance of a heat pump improves with increasing source temperatures; this can be affirmed from the plot. For both normal and smart operation modes, the PFs of the heat pump for DHW operation increase with rising ambient temperatures. However, the performance factors during SG-Ready OS3 are lower than those during normal OS2, as the SG-Ready control intensifies the heat pump operation by increasing the supply temperatures.

Without differentiating between the different operation modes (OS2 and OS3) the annual SPF for DHW productions amounts to 3.3. To quantify the effect of the SG-Ready control on HP's efficiency different approaches will be introduced hereafter.

The first approach addresses the efficiency difference for ambient temperatures between 0 °C and 35 °C, where the heat pump operation in both, OS2 and OS3 occurs. To neglect the influence of weighting the PF with the corresponding energies, either during high or low ambient temperatures, only the regression curves of the PF values for each mode are considered and the average PF difference amounts to 0.42 points. This can be understood as, the OS3 reduced the PF for DHW by 0.42 points when calculated based on the average difference from the regression curve. In contrast, when considering the corresponding energies produced in OS2 and OS3, i.e., weighting the PFs per bin from the regression curve with the thermal energy produced, the PF difference from regression curves amounts to 0.26. The reduced difference is due to the fact that most of the OS2 occurs at lower ambient temperatures as compared to OS3. As mentioned, operation with different ambient temperature entails also different source temperatures and thus different efficiencies.

Another, yet more comprehensive approach includes calculating the PF by neglecting the existence of OS3. This approach assumes that all the thermal energy is produced under the operating conditions of OS2; correspondingly the PF is calculated by weighting the PFs for OS2 with the total thermal energy generated for DWH. Assuming that for both operation modes the same source temperatures per ambient temperature bin occur, the influence of the source temperatures can be excluded. By weighting the PF in OS2 with the total thermal energy produced during OS3, a SPF is of 3.5 can be calculated. When compared to the actual SPD of 3.3 for DHW, it can thus be concluded that owing to higher supply temperatures in OS3, a reduction of DSPF3 = 0.2 points for DHW operation can be observed.3.4.2 Effect of PV-optimized HP control on space heating mode

For space heating, the supply and return temperatures per heat pump cycle, and the corresponding hourly performance factors, separated for

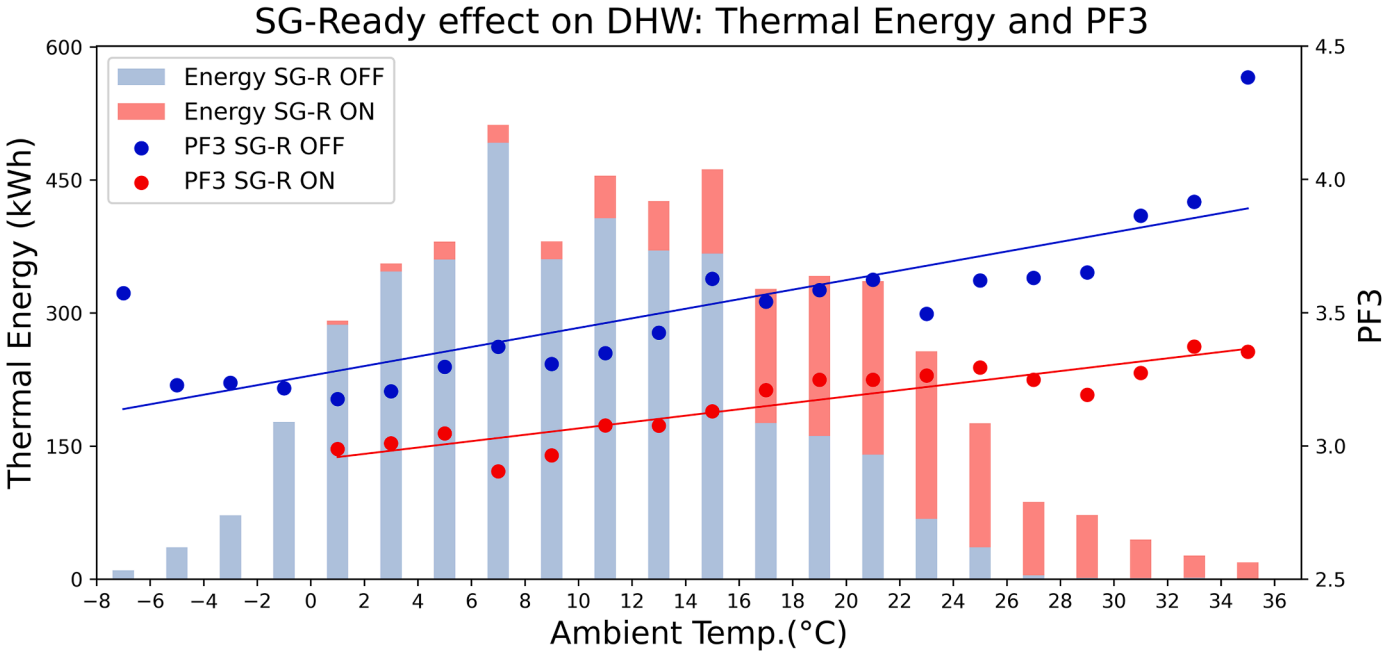


**Fig. 11.** Heat pump thermal energy generation for DHW and the corresponding PF3 per 2 K bin of ambient temperature.

normal and smart operation are depicted in Fig. 12. For OS2, the heating curve (blue and green points for supply and return temperatures respectively) ranged from around 46 °C supply temperature at the lowest operation point of about −7 °C ambient temperature to around 40 °C at an ambient temperature of 16 °C. However, space heating occurred additionally under SG-Ready OS3 mode (red and orange points for supply and return temperatures respectively) up to an ambient temperature of 19 °C. Two distinct curves were observed for OS2 operation of the heat pump, which upon investigation were found to be a result of nighttime reduction between 02:00 AM to 05:00 AM, employed as an energy-saving measure. A slight shift of the heating curve is seen over the entire operation range which is a result of SG-Ready control (red curve) increasing the heat pump supply temperature, as compared to the curve in normal operation (blue curve). The annual thermal energy weighted supply temperature for space heating is 38.8 °C. Separated for normal and smart operation modes, the thermal energy weighted supply temperatures are 38.9 °C for operation in OS2 and 39.2 °C in OS3, a temperature rise of $\Delta T_{supply} = 0.3$ K. To determine the instantaneous temperature rise set in the control further analysis of regression curves for the supply temperatures in OS2 and OS3 between ambient temperatures of 0 °C and 16.4 °C were done. This temperature range was chosen as both, OS2 and OS3 occurred during this range, which makes the comparison more sensible. The average difference of both curves amounts to 1.8 K.

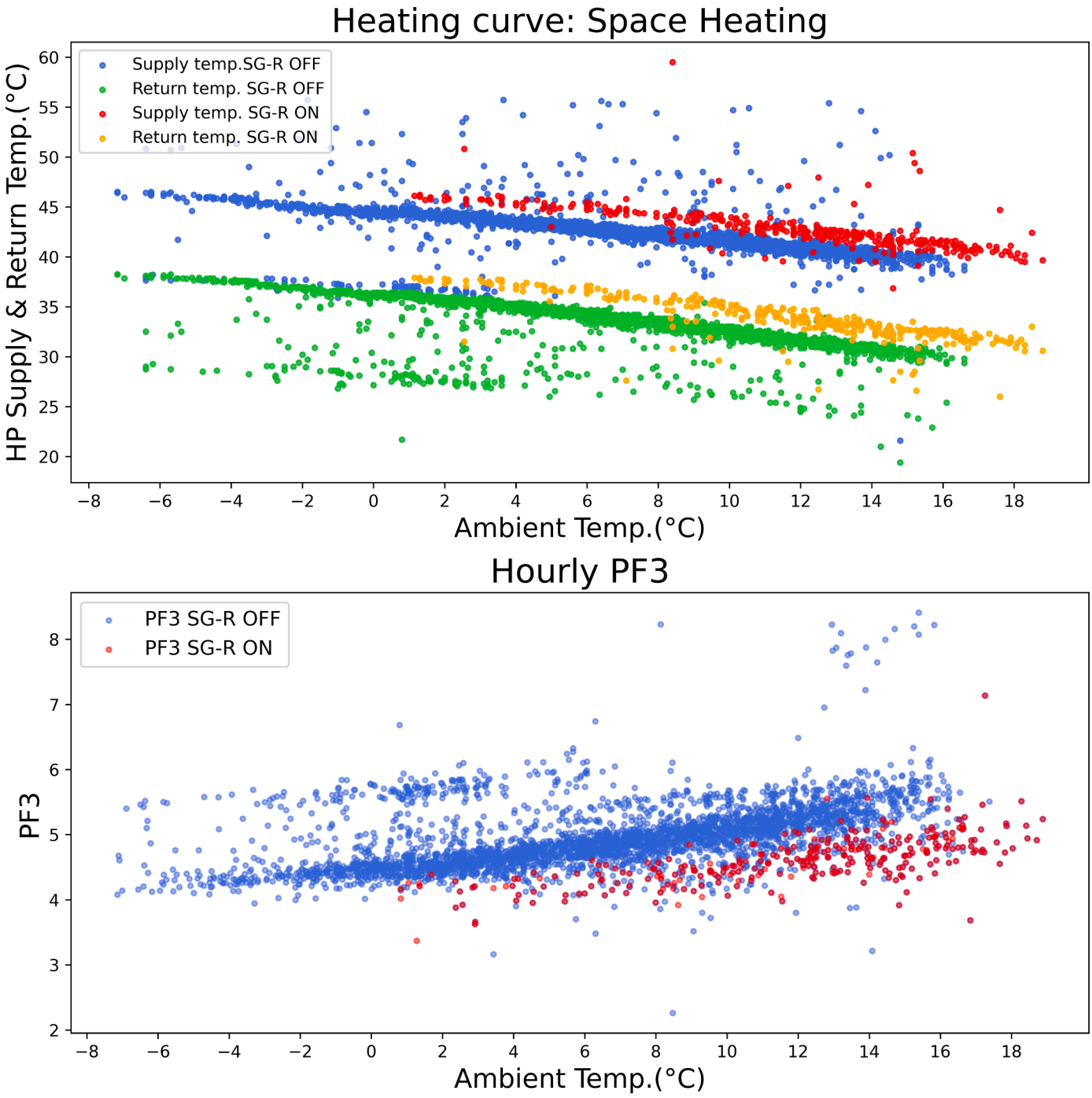


**Fig. 12.** Measured heating curve with maximum supply and return temperatures per heat pump cycle vs ambient temperature (top) and hourly PF3 vs. ambient temperature (bottom) for space heating; separated for normal and SG-Ready controlled operation.

The graph at the bottom shows the hourly performance factors of the heat pumps against ambient temperature. According to basic thermodynamical relations a distinct positive linear relation is seen between the performance factors and the outside temperature. It is also apparent that the increase in supply temperatures in the SG-Ready operation reduces the performance efficiency of the heat pump. A better interpretation of this effect of smart control is depicted in Fig. 13.

The heat pump produced 16,260 kWh for space heating over the entire observation period. Compared to DHW mode (26 %) the SG-Ready OS3 for space heating occurred significantly less due to lower radiation in the heating period. Only 5 % or 814 kWh of the thermal energy for space heating was produced during OS3, distinguished by the red section of the bars in Fig. 13 respectively. Nevertheless, the overall covering of the space heating mode by PV/battery electricity is significantly higher since the solar fraction for space heating amounts to 0.28. The SG-Ready controlled operation for space heating only occurred at ambient temperatures above 0 °C. Interestingly, above the outside temperature of 16.5 °C, the heat pump operated shortly and solely under smart operation mode. As also apparent form the heating curve (Fig. 12), without the influence of OS3, this additional operation of the heat pump for space heating might not have occurred.

The corresponding PFs for the two operation modes are shown by the blue markers for OS2 and by the red markers for OS3. Both the PFs follow an upward trend, with increasing outdoor temperatures.

Without separating for the OS2 and OS3 modes, the annual performance factor, calculated as the mean of thermal energy weighted PF per bin, is found to be 4.8 for space heating operation of the heat pump. Approaches, analogous to the ones introduced in Section 3.4.1, are described for space heating, to quantify the effect of SG-Ready control on the heat pump's efficiency, as follows.

The approach in which only considering ambient temperatures between 0 °C and 16.5 °C, and the regression curves of the PF values results in an average PF difference of 0.65 points. Considering additionally the corresponding energies produced in SG-Ready OS2 and OS3 the PF difference lowers to 0.42 points. The reduction in the PF difference is because most of the OS2 occurred at lower ambient temperatures, and thus, at lower source temperatures as compared to OS3. Additionally, in contrast to DHW, here the effect is more prominent also because of the higher supply temperatures in OS2 governed by the heating curve.

For the more comprehensive approach with weighting the PF in OS2 with the total thermal energy produced during OS3, a SPF3 of 5.0 can be calculated. This translates to a reduction of $\Delta SPF3 = 0.2$ points due to OS3, for space heating operation compared to the actual SPF3 of 4.8.

## 4. Discussion

The coupling of heat and electricity in buildings, in the form of PV-HP-battery systems is emerging as an all-round solution in the residential market. Supplying highly efficient heat pumps with renewable domestic PV electricity adds to not only the ecological, but also economic benefits from a homeowner's perspective. In the financial context, it is favorable for homeowners to maximize their PV self-consumption because of the high-and-rising grid electricity prices for purchased electricity from the grid. A further potential lies in optimizing the heat pump operation by implementing smart control strategies to operate the heat pump in a PV-oriented way. This section discusses the evaluation outcomes of such PV-HP-battery system evaluated under the scope of this work.

- How do the PV and battery units affect the performance of the "solar heat pump system"?

To answer this question, system boundaries are defined on the electrical input side of the heat pump, for the same thermal output across all the boundaries. This methodology is similar to solar-thermal heat pump systems, where the heat supplied by the solar thermal unit can reduce the heat pump demand. However, in PV-HP systems, the benefits are in the form of reduced grid consumption which also reduces electricity costs [17]. Accordingly, boundary $SB_{HP}$ refers to an assumed case where the complete electricity consumption of the heat pump is supplied by the grid. The corresponding $SPF3_{HP}$ can be understood as the common SPF3 of the system. The system has an annual $SPF3_{HP}$ of 4.2. Subtracting the PV power directly consumed by the heat pump ($SB_{HP+PV}$), the corresponding $SPF3_{HP+PV}$ increases to 5.2, indicating an extra kWh of thermal output compared to $SB_{HP}$. With the addition of a battery storage unit, the $SPF3_{HP+PV+BAT}$ increases to 6.7. With an analogous interpretation to the above case, this indicates that by considering the direct consumption of total (PV+battery) self-generated

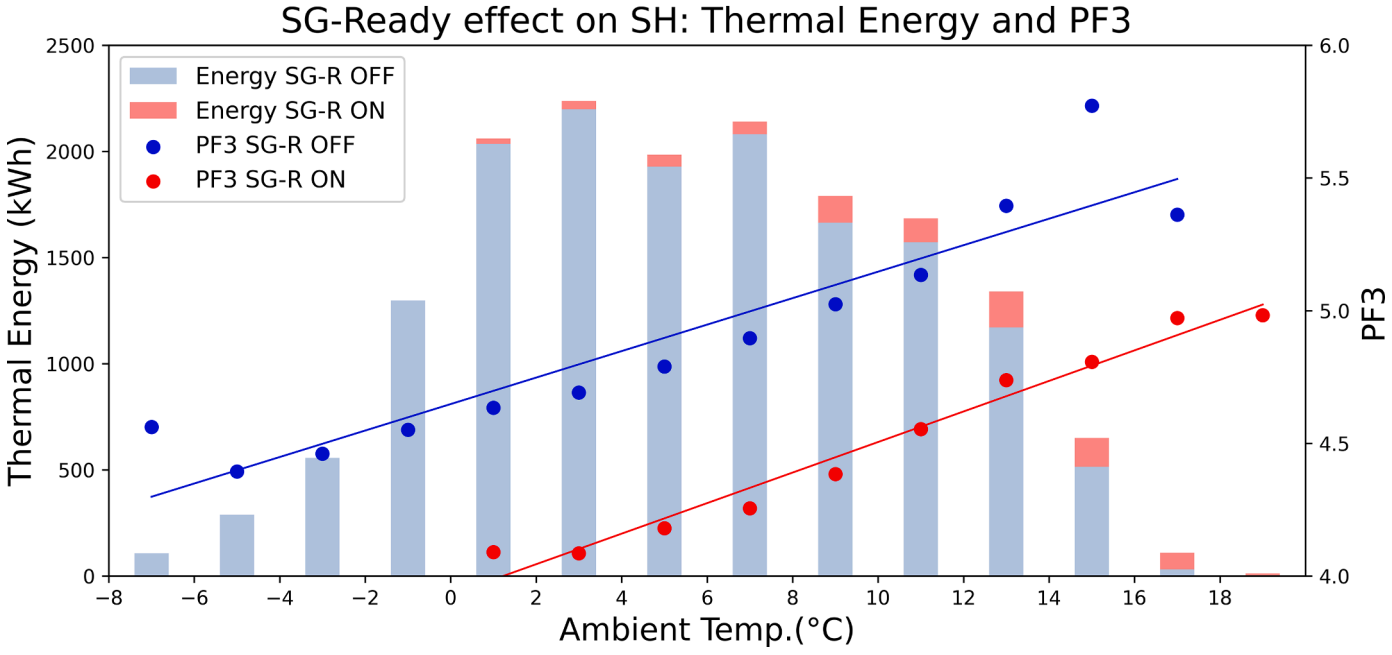


**Fig. 13.** Heat pump thermal energy generation for space heating and the corresponding PF3 per 2 K bin of ambient temperature.

electricity, the user gets 6.7 kWh of thermal energy for each kWh purchased from the grid.

The increase in the performance factors by considering the self-consumption of PV and PV+battery is indicative of a high significance of self-generated electricity in supplying the heat demand of the building heating system. From a homeowner's perspective, this can be interpreted as direct cost savings in the electrical consumption for building heating, and independence from the grid. However, the high efficiency as presented by $SPF3_{HP+PV}$ and $SPF3_{HP+PV+BAT}$ must not be mistaken with the actual annual SPF of the heat pump. The SPF is a measure of the efficiency of the heat pump in transferring heat from a source to a sink, by consuming external power. On the other hand, the three variations discussed above are a theoretical consideration, aimed at indicating the potential benefits of adding PV and battery to the building's energy system, and their contribution in the heat pump's electricity consumption. It is important to look at these KPIs along with the actual absolute values of the contribution of the PV and battery in the heat pump's electricity consumption. Moreover, their values stated in this work are only valid for the given system configuration and may change significantly depending on factors such as the size of PV and battery units, household consumption load profile, the HP's load profile, the solar irradiation and applied system control strategy among others. Furthermore, this work assumed the PV and battery electricity as free sources of electricity and calculated the SPF3 for only the grid input. In reality, both the battery and PV units come with their respective economic and ecological costs. The PV and battery systems cannot be considered completely free, till their payback periods are reached. A complete life cycle analysis will give a better idea of the actual ecological and economic savings by the self-generation of electricity. Furthermore, from an ecological perspective, the share of renewable energy in the grid electricity should also be considered.

In addition to the efficiency improvements from the use of PV/battery power, few disadvantages must be mentioned. The direct influence of the temperature increase on the HP efficiency is discussed below. However, what is not quantified in the present work are the additional heat losses of the buffer storages for space heating and DHW as well as possibly unnecessary operation of the heat pump due to the temperature increase. At least the operation in space heating mode above the heating-threshold temperature could be detected in the heating curve analysis (Fig. 12).

Over the complete year, the system has a self-consumption of 42.9 %. This value is within the normal range of 30 % to over 65 % as specified in literature [16]. Self-consumption is highly governed by the available PV power, with values close to 100 % during January, November, and December. In contrast, high surplus PV leads to lower self-consumption in summer, typically during the peak sunlight hours. Larger battery capacity would help to maximize the self-consumption; however, this also implies that most of the battery capacity would be left unused during the winter months with limited PV surplus power. The battery is set to charge whenever PV surplus is available, depending on the sequence logic, which indicates the self-consumption-optimized strategy, common for residential systems [16]. Moreover, is it also seen the solar fraction of the system greatly follows the PV generation pattern. A solar fraction of SF = 0.36 is recorded over the year. Values between SF = 0.25 to 0.40 are reported in literature in the German context [16].

- How does the smart control affect the operation behavior and efficiency of the heat pump?

A distinct SG-Ready signal is read out by the measurement equipment which helps distinguish the performance of the system under normal (OS2) and forced (OS3) operation. Particularly, when the control strategy is set to modify system set-point temperatures, this can be precisely captured by the measured temperatures. Since the set parameters are not known, the temperature increases from OS2 to OS3 were determined using regression lines of the measured supply temperatures per operating mode. In space heating mode the temperature increase was 1.8 K and in domestic hot water mode 4.1 K. However, both operating modes differ significantly in how often OS3 was applied. While in the space heating mode only 5 % of the thermal energy was provided at raised temperatures, in the domestic hot water mode it was 28 %. The influence on the efficiency in the water heating mode is correspondingly higher. The temperature increase reduces the efficiency of 3.5 by 0.2 points and thus by 5.7 %. In space heating mode, the efficiency is reduced from 5.0 to 4.8 and thus by only 4.0 %. That the different temperature raises and energy shares per operating mode in OS3 suggest an even greater influence needs further investigation. A possible approach would be the influence by the individual characteristic curves of the coefficient of performance at different source and sink temperatures, since both are in very different ranges during OS3. Moreover, due to the pure field-based approach for the analysis, simplifications in the evaluation methodology and existing measurement errors must be taken into account.

## 5. Conclusion

Acting as an important connector, heat pumps enhance the integration and collaboration between the heat and electricity sectors. This work highlights the significance of combined operation of heat pump and PV+battery systems in terms of self-consumption level, solar fraction, efficiency of the heat pump, and the effect of PV+battery units on the heat pump performance efficiency. High-resolution 1-minute data from January to December 2022, from a PV-HP-battery system in a single-family household in Germany is analyzed to evaluate the system combination. The synergies between PV, heat pump, and battery systems were analyzed using field measurement data to derive KPIs specific to PV-HP systems.

A discrete SG-Ready control signal was read out by the measurement equipment. The findings show that SG-Ready control of the heat pump increased the heat pump supply temperatures by 4.1 K for DHW, and by 1.8 K for space heating to maximize the PV self-consumption. The system had an overall self-consumption of 42.9 % for the year analyzed. The electricity demand for the HP was covered by 36 % with the PV/battery system, through 51 % in domestic hot water mode and 28 % in space heating mode. Due to higher sink temperatures the HP's efficiency decreases by 5.7 % in DHW mode and by 4.0 % in space heating mode.

The study also evaluated the impact of PV and battery storage on the electricity demand of the heat pump system. This was performed by redefining the system boundaries in line with current literature. The aim was to assess the heat pump system performance for only the grid electricity consumed. Results showed that by considering the PV electricity supplied to the heat pump, the SPF3 increased from 4.2 to 5.2. When the combined supply from PV and battery to the heat pump was considered, the SPF3 increased to 6.7. These SPFs give the amount of heat output for each kWh of grid electricity supplied to the heat pump depending on their source. In simpler terms: the benefit lies in the reduced grid electricity needed to meet the household heating demands. However, it must be noted that these findings are specific for the individual evaluated systems and can vary greatly depending on the building and energy system specifications. Limited number of studies have analyzed this approach for evaluating a PV-HP-battery system combination.

Overall, the results highlight the benefits of integrating PV, battery, and heat pump systems to achieve better energy performance of the household. The resulting higher self-consumption translates to financial benefits for the homeowners. Nevertheless, the smart control can have a negative effect on the heat pump efficiency due to increased supply temperatures. Long-term evaluation at the system level, by considering the effect of storage losses and considering the economic performance can better assess the effect of smart control on the system. Moreover, the PV and battery units significantly enhance the performance of the heat pump, calculated based on grid electricity consumption. With the focus

on heating systems, future work should consider a wholistic approach by analyzing the economic and ecological impact of this system combination, by following a standard set of system boundaries. As part of the "WP-QS im Bestand" project, up to nine additional PV/HP combinations with different system and control concepts will be evaluated in an identical manner by mid-2024.

## 'Declaration of generative AI and AI-assisted technologies in the writing process'

Statement: During the preparation of this work the authors used ChatGPT in order to improve the quality and readability of text. After using this tool/service, the authors reviewed and edited the content as needed and take full responsibility for the content of the publication.

## Declaration of Competing Interest

The authors declare that they have no known competing financial interests or personal relationships that could have appeared to influence the work reported in this paper

## Acknowledgments

We gratefully acknowledge financial support of the German Federal Ministry for Economic Affairs and Energy (BMWK) due to an enactment of the German Bundestag under grant numbers 03EN2029A ("WP-QS im Bestand") [29]. We would like to thank all project partners for the fruitful cooperation.

## Appendix

**Table A.1**
Thermal and electrical parameters read by the DAQ unit.

| Thermal energy | Electrical energy | Temperature |
|---|---|---|
| HP output (space heating and DHW) | Electrical grid | Ambient air |
| Ground source | PV generation | HP source (flow and return) |
| Space heating circuit (after storage) | Battery | HP supply (flow and return) |
| DHW circulation | Building load | Space heating after storage (flow and return) |
| DHW tapping | Compressor + controls | DHW circulation (flow and return) |
| – | Auxiliary heater (space heating) | DHW tapping (flow and return) |
| – | Auxiliary heater (DHW) | – |
| – | Brine pump | – |
| – | Space heating loading pump | – |
| – | Heating circuit pump (after storage) | – |
| – | DHW loading pump | – |
| – | DHW circulation pump | – |

**Table A.2**
Details of the measurement equipment.

| Parameter | Sensor type | Standard |
|---|---|---|
| Ambient temp | Pt100 | IEC 60751 Class B |
| HP flow and return temp. | Pt500 | EN 1434 class 2 |
| HP volume flow | Ultrasonic | EN 1434 class 2 |
| HP source flow and return temp. | Pt500 | EN 1434 class 1 |
| HP source volume flow | MID | EN 1434 class 1 |
| Electric meters | – | IEC 62053–21 class B |

**Table A.3**
Operating conditions assumed for the error calculation.

| Measuring Instrument | Value | Number | Unit |
|---|---|---|---|
| Heat Meter | Temperature Difference | 5.0 | K |
| | Volume Flow | 1.05 | $m^3/h$ |
| | Operation Time | 1800 | h |
| Electrical Meter | Electrical Work | 2600 | kWh |

**Table A.4**
Initial values and the results for relative and absolute errors of the partial values and the resulting SPF 3.

| Value | Formula symbol | Error limit | Measured value | Unit | Absolute Error | Relative Error |
|---|---|---|---|---|---|---|
| Temperature Difference | dT | $E_t$ | 5.0 | K | 0.12 | 2.3% |
| Volume Flow | | $E_V$ | 1.05 | $m^3/h$ | 0.03 | 3.0% |
| Heat Capacity Water | $c_p$ | $E_C$ | 4186.0 | J/(kg*K) | 46.05 | 1.1% |
| Density Water | ρ | $E_C$ | 998.2 | $kg/m^3$ | 10.98 | 1.1% |

(continued on next page)

**Table A.4** (*continued*)

| Value | Formula symbol | Error limit | Measured value | Unit | Absolute Error | Relative Error |
|---|---|---|---|---|---|---|
| Electrical Energy | $E_{el}$ | $E_P$ | 2600.0 | kWh | 52.00 | 2.0% |
| SPF 3 | SPF3 | – | 4.2 | – | 0.19 | 4.4% |

**Table A.5**
Electricity sources and sinks to verify power balance in the evaluated system.

| Sources | Sinks |
|---|---|
| PV generation | Household + TBE* consumption |
| Battery discharge | Battery charge |
| Grid supply | Grid feed-in |

* TBE refers to the technical building equipment such as compressor, heating circuit pumps, measurement equipment, circulation pumps, control system, etc.

**Table A.6**
Electrical and thermal components included in the system boundary 3.

| | ASHP | GSHP |
|---|---|---|
| Thermal output | Compressor ($Q_{th.HP}$) | |
| | Auxiliary heater ($Q_{th.aux}$) | |
| Electrical input | Compressor ($E_{el.comp}$) | Compressor ($E_{el.comp}$) |
| | Auxiliary heater ($E_{el.aux}$) | Auxiliary heater ($E_{el.aux}$) |
| | Fan ($E_{el.fan}$) | Brine pump ($E_{el.brinepump}$) |
| | Control ($E_{el.ctrl}$) | Control ($E_{el.ctrl}$) |

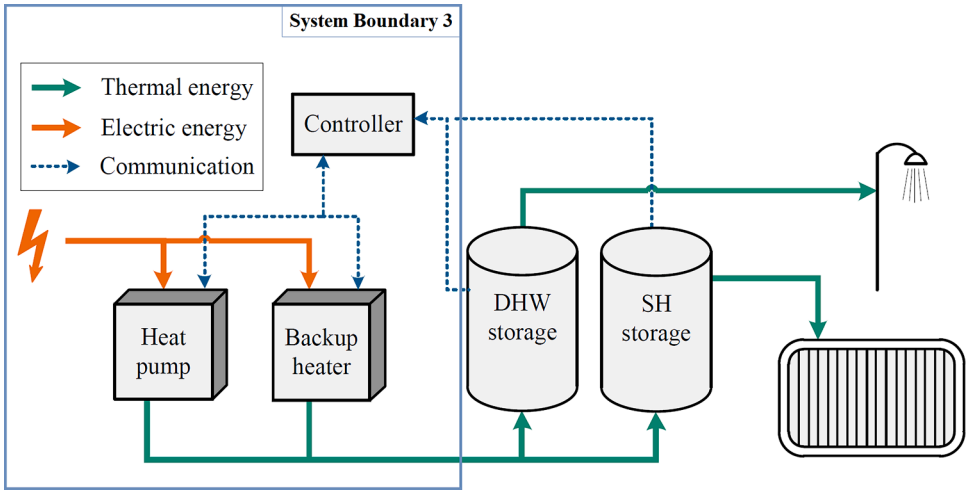


**Fig. A.1.** System boundary 3 for heat pump systems. Figure adapted from [30].

## References


[1] Deutsche Energie-Agentur GmbH (dena), German Energy Agency, No energy transition without a heating transition. [Online]. Available: https://www.dena.de/en/topics-projects/energy-efficiency/buildings/ (accessed: Apr. 14 2023).

[2] Federal Statistical Office, Electricity consumption of households by household size. [Online]. Available: https://www.destatis.de/EN/Themes/Society-Environment/Environment/Environmental-Economic-Accounting/private-households/Tables/electricity-consumption-private-households.html (accessed: Apr. 3 2023).

[3] Bundesministerium für Wirtschaft und Klimaschutz, Neue Heizungen sollen ab 2024 auf Erneuerbare setzen. [Online]. Available: https://www.bmwi-energiewende.de/EWD/Redaktion/Newsletter/2023/03/Meldung/direkt-erfasst.html (accessed: Apr. 27 2023).

[4] BMWK and BMWSB, 65 Prozent erneuerbare Energien beim Einbau von neuen Heizungen ab 2024: konzeption zur Umsetzung (accessed: Apr. 24 2023).

[5] Bundesverband Wärmepumpe (BWP) e.V, Wärmepumpenabsatz 2022: wachstum von 53 Prozent gegenüber dem Vorjahr. Berlin, 2023. Accessed: Apr. 10 2023.

[6] S.Philipps, W. Warmuth et. al., Photovoltaics Report, Fraunhofer institute for Solar Energy Systems and PSE Projects GmbH, Last updated: 2023, Available: https://www.ise.fraunhofer.de/en/publications/studies/photovoltaics-report.html.

[7] J. Weniger, T. Tjaden, V. Quaschning, Sizing of residential PV battery systems, Energy Procedia 46 (2014) 78–87, https://doi.org/10.1016/j.egypro.2014.01.160.

[8] B. Wehrmann (April 1st 2023), What German households pay for electricity, Available: https://www.cleanenergywire.org/factsheets/what-german-households-pay-electricity.

[9] A. Zeh, R. Witzmann, Operational strategies for battery storage systems in low-voltage distribution grids to limit the feed-in power of roof-mounted solar power systems, Energy Procedia 46 (2014) 114–123, https://doi.org/10.1016/j.egypro.2014.01.164.

[10] W. Hennings, P. Stenzel, N. Pflugradt, Performance of a photovoltaic plus battery home system with load profile scenarios changing over the system life, Energy Procedia 142 (2017) 3252–3257, https://doi.org/10.1016/j.egypro.2017.12.499.
[11] E. Nyholm, J. Goop, M. Odenberger, F. Johnsson, Solar photovoltaic-battery systems in Swedish households—self-consumption and self-sufficiency, Appl. Energy 183 (2016) 148–159, https://doi.org/10.1016/j.apenergy.2016.08.172.
[12] J. Widén, J. Munkhammar, Evaluating the benefits of a solar home energy management system: impacts on photovoltaic power production value and grid interaction, in: ECEEE SUMMER STUDY Proceedings, 5A. Cutting the Energy Use of Buildings: Projects and Technologies, 2013.
[13] T. Tjaden, F. Schnorr, J. Weniger, J. Bergner, V. Quasching. Einsatz von PV-Systemen mit Wärmepumpen und Batteriespeichern zur Erhöhung des Autarkiegrades in Einfamilienhaushalten, Hochschule für Technik und Wirtschaft (HTW) Berlin, 30. Symposium Photovoltaische Solarenergie, March 4th to 6th, Kloster Banz, 2015. Bad Staffelstein.
[14] A. Hadeier and A. Widmann, "C.A.R.M.E.N. - Marktübersicht Batteriespeicher: Marktübersicht Batteriespeicher 2022 - Auswertung," C.A.R.M.E.N. e.V., 2022.
[15] J. Munkhammar, P. Grahn, J. Widén, Quantifying self-consumption of on-site photovoltaic power generation in households with electric vehicle home charging, Sol. Energy 97 (2013) 208–216, https://doi.org/10.1016/j.solener.2013.08.015.
[16] D. Fischer, H. Madani, On heat pumps in smart grids: a review, Renew. Sustain. Energy Rev. 70 (2017) 342–357, https://doi.org/10.1016/j.rser.2016.11.182.
[17] S. Poppi, N. Sommerfeldt, C. Bales, H. Madani, P. Lundqvist, Techno-economic review of solar heat pump systems for residential heating applications, Renew. Sustain. Energy Rev. 81 (2018) 22–32, https://doi.org/10.1016/j.rser.2017.07.041.
[18] E.-L. Niederhäuser, N. Huguelet, M. Rouge, P. Guiol, D. Orlando, Novel approach for heating/cooling systems for buildings based on photovoltaic-heat pump: concept and evaluation, Energy Procedia 70 (2015) 480–485, https://doi.org/10.1016/j.egypro.2015.02.151.
[19] Maria Pinamonti, Alessandro Prada, Paolo Baggio, Rule-based control strategy to increase photovoltaic self-consumption of a modulating heat pump using water storages and building mass activation, Energies 13 (2020), https://doi.org/10.3390/en13236282.
[20] M. Battaglia, R. Haberl, E. Bamberger, M. Haller, Increased self-consumption and grid flexibility of PV and heat pump systems with thermal and electrical storage, Energy Procedia 135 (2017) 358–366, https://doi.org/10.1016/j.egypro.2017.09.527.
[21] Smart Control Strategy for PV and Heat Pump System Utilizing thermal and electrical storage and forecast services. ISES Solar World Congress, 2017.
[22] Flexibility of heat pump pools, The use of SG-Ready from an aggregator's perspective, in: 12th IEA Heat Pump Conference, Rotterdam, 2017.
[23] D. Zenhäusern, "Key performance indicators for PVT systems," 2020.
[24] C. Fraga, P. Hollmuller, S. Schneider, B. Lachal, Heat pump systems for multifamily buildings: potential and constraints of several heat sources for diverse building demands, Appl. Energy 225 (2018) 1033–1053, https://doi.org/10.1016/j.apenergy.2018.05.004.
[25] M. Koch, "Regularium: für das Label „SG Ready" für elektrische Heizungs- und Warmwasserwärmepumpen und kompatible Systemkomponenten," Berlin, 2020.
[26] Fraunhofer-Institut für Solare Energiesysteme ISE, WPsmart im Bestand: Wärmepumpenfeldtest – Fokus Bestandsgebäude und smarter Betrieb - Fraunhofer ISE. [Online]. Available: https://www.ise.fraunhofer.de/de/forschungsprojekte/wpsmart-im-bestand.html (accessed: Sep. 20 2023).
[27] H. Madani, J. Claesson, P. Lundqvist, A descriptive and comparative analysis of three common control techniques for an on/off controlled Ground Source Heat Pump (GSHP) system, Energy Build. 65 (2013) 1–9, https://doi.org/10.1016/j.enbuild.2013.05.006.
[28] M. Lämmle, et al., Performance of air and ground source heat pumps retrofitted to radiator heating systems and measures to reduce space heating temperatures in existing buildings, Energy 242 (2022), https://doi.org/10.1016/j.energy.2021.122952.
[29] Fraunhofer-Institut für Solare Energiesysteme ISE, WP-QS im Bestand – Entwicklung optimierter Versorgungskonzepte und nachhaltiger Qualitätssicherungsmaßnahmen für Wärmepumpen im EFH-Bestand - Fraunhofer ISE. [Online]. Available: https://www.ise.fraunhofer.de/de/forschungsprojekte/wp-qs-im-bestand.html (accessed: Apr. 15 2023).
[30] D. Fischer, T. Wolf, J. Wapler, R. Hollinger, H. Madani, Model-based flexibility assessment of a residential heat pump pool, Energy 118 (2017) 853–864, https://doi.org/10.1016/j.energy.2016.10.111.